Available online at www.CivileJournal.org

Civil Engineering Journal

(E-ISSN: 2476-3055; ISSN: 2676-6957)

Vol. 12, No. 01, January, 2026

Flood Simulation Utilizing HEC-HMS and HEC-RAS

Yasameen T. Yousif [1*], Ahmed N. A. Hamdan [1]

[1] *Department of Civil Engineering, College of Engineering, University of Basrah, P.O. Box 49, Basrah, Iraq.*

Received 23 August 2025; Revised 10 December 2025; Accepted 14 December 2025; Published 01 January 2026

Abstract

The substantial amount of rainfall leading to runoff in floodplain regions poses hazards to residents within these areas and surrounding zones; consequently, flood simulation is crucial for precise risk evaluation and the formulation of water utilization strategies. In this research, hydraulic and hydrological models, supported by Geographic Information Systems (GIS), were employed to simulate rainfall-runoff mechanisms in Wasit Governorate, central Iraq. A resolution of 30 m Digital Elevation Model (DEM) was supplied by the USGS, geospatially processed, and then imported into the Hydrologic Modeling System (HEC-HMS) at the Hydrologic Engineering Center. The runoff within the research area was estimated using the SCS-CN approach. In order to find the Curve Numbers (CN), a number of datasets were combined, including those pertaining to land use, land cover (LULC), and soil types. The HEC-HMS system was fed CN values obtained from GIS, which varied between 73.95 and 97.61. During the incident in November 2015, the Hydrologic Engineering Center's River Analysis System (HEC-RAS) was utilized to simulate floods using the runoff data resulting from HEC-HMS. Inundation maps were produced using RAS-Mapper within HEC-RAS, depicting flood depth and velocity through the study area. The flood model underwent calibration through comparison of the simulation results with satellite imagery for November 14, 2015. Using CSI, the hydrological factors Ia, Muskingum K, and X, and impervious % were adjusted using sensitivity analysis to achieve the greatest convergence between the model and satellite image. The result of CSI was 88.56%, (HR) was 96.31%, and (FAR) was 8.33%. The validation has been done for the calibrated parameters, and the results were compared with satellite imagery for April 3, 2019. The high level of concordance allowed for the final inundation map to be approved. The importance of measuring runoff for managing water resources effectively and reducing flood risks is highlighted by this study.

Keywords: Rainfall-Runoff Modeling; Hydrologic Simulation; River Flow Modeling; Hydraulic Model; HEC-RAS; HEC-HMS.

1. Introduction

During heavy rainfall events in western Iran, substantial runoff flows into eastern Iraq. The Wasit Governorate, located in eastern Iraq, experiences a significant amount of this runoff, leading to flooding that endangers lives and property. One non-structural method to minimize damage and flood risk is flood estimation through hydrological and hydraulic development. A significant probability of flood recurrence was suggested by statistical analysis of yearly rainfall data at the Badra, Sumer, Kut, Ilam, and Mehran stations (2000-2020), with return periods of 2-50 years [1]. The flood's intricacy makes its total prevention an impossibility. Accurate knowledge of flood-expanded areas and effective flood hazard management measures, however, may greatly mitigate its effects. Since the Tigris and Euphrates rivers get less recharge during dry seasons, flood prediction is crucial in Iraq. Because of their enormous volume, the floodwaters might be collected and used to recharge groundwater recharge supplies or feed the Tigris River. Flood risk assessment, which includes flood mapping and identifying regions prone to flooding, is the starting point of any plan for managing floods.

* Corresponding author: yasameen.yousif@uobasrah.edu.iq

https://doi.org/10.28991/CEJ-2026-012-01-013

The geographical distribution of inundation patterns—including water depth, flow, and velocity—can be better understood with the help of flood inundation modeling. It is crucial to use hydraulic modeling software such as HEC-RAS and GIS tools for flood risk assessments, non-structural techniques, and flood inundation mapping in order to be ready to deal with repeated high-level floods [2].

In November 2015, October 2018, and April 2019, several Iraqi cities experienced widespread flooding, with 2019 being the most severe flood year within that interval [3]. This underscores that the study area was among the most affected regions during that period. Flood mapping is primarily performed using hydrologic/hydraulic models. Hydrological and hydraulic modeling depend on mathematical and theoretical foundations, which were developed to understand the behavior of the spatial and temporal distribution of rainfall and runoff [4]. Their main applications include flood management planning, flood risk estimation, flood simulation, and identification of relevant geographically distributed variables. The dynamics of fluid motion and flood waves are commonly described by mathematical equations that are solved using the laws of mass conservation and momentum.

The US Army Corps of Engineers' Hydrologic Engineering Center (HEC) has created a number of cutting-edge hydrologic and hydraulic modeling methods to supplement spatial assessments. The HEC-Hydrologic Modeling System (HEC-HMS) is one such instrument; it can model dendritic watershed systems' precipitation-runoff processes. It has several potential uses in solving hydrologic issues. Studies on flood hydrology and water supply in big river basins [5]. Similarly, the HEC-River Analysis System software (HEC-RAS) was developed to perform one- or two-dimensional unsteady or steady flow conditions analysis. While one-dimensional models effectively simulate streamflow processes, two-dimensional models are more suitable for analyzing floodplain dynamics, especially when water overflows from streams and spreads across downstream areas. Two-dimensional models are widely used for flood mapping and hazard prediction due to their high accuracy in complex flow simulations. Despite their computational intensity, two-dimensional models that fully solve shallow water equations provide accurate simulations of flood timing and duration. Studies on flood insurance and floodplain management often utilize HEC-RAS models to assess the effects of floodway encroachments [6].

The HEC-HMS model is used in some of the global investigations. Hydrographic and flood peak predictions using the model have been validated in several investigations. Salman & Hamdan [7] developed a hydrological model for the central region of the Lesser Zab River (LZR) watershed in Iraq, using HEC-GeoHMS, HEC-HMS, and GIS tools. The model applied the SCS-Curve Number technique, the SCS Unit Hydrograph, the Muskingum method, and the Recession method. The study found that the CN parameter was the most sensitive input, highlighting the effectiveness of integrating GIS with HEC-HMS in simulating runoff in data-scarce regions. Olayinka & Irivbogbe [8] performed a study to investigate the runoff process in areas surrounding LGAs, including Lagos Island and Eti-Osa Local Government Areas, using GIS with the HEC-HMS hydrological model to simulate it. The SCS-CN technique was used for loss estimation and verified the accuracy of simulated peak discharges during known flood events. The results show the model's ability to support the development of early flood warning systems. Sagathia et al. [9] and Hamdan et al. [10] utilized HEC-HMS in conjunction with HEC-GeoHMS and ArcGIS to simulate flow through rainfall-runoff processes. Hydrological methods employed in these studies include the SCS-Curve Number for losses, as well as the Muskingum and unit hydrograph methods for flow routing and transformation, respectively. The model was calibrated and validated using discharge data in the study area. The results from both studies indicate that hydrological simulations in semi-arid to urban fringe environments can be effectively achieved with this model. Kazezyılmaz-Alhan et al. [11] used the HEC-HMS model to create a hydrological model of the Ayamama watershed in Istanbul, which allowed them to reproduce a big flood that happened on September 9, 2009. Green-Ampt, Clark Unit Hydrograph, and kinematic wave modeling were used to capture the hydrological processes. Results demonstrated strong agreement when compared to a previously calibrated model that used the Rational Method in the Watershed Modelling System (WMS).

Around the globe, researchers have used the 2D HEC-RAS model in a number of studies. Multiple studies have used the model to accurately forecast flood hydraulic models. Hamdan et al. [12] utilized 2D HEC-RAS to model a flood in the Shatt Al-Arab River in southern Iraq owing to a planned barrage. The results suggest the regulator's construction with certain precautions. Afzal et al. [13] predicted river dynamics during severe flow events and inundation modeling using HEC–RAS. The 2010 and 2015 floods were used to calibrate and validate the HEC–RAS v5 model. Land use data from rivers and floodplains was used to calculate Manning's roughness coefficient (n). This research found that the HEC–RAS v5 model plus satellite images might be utilized for early flood warnings in the middle Indus River basin. Mohamed et al. [14] investigated and assessed flood wave characteristics when Mosul Dam in northern Iraq broke owing to pipe failure. The research revealed that the 2D HEC-RAS model can analyze and simulate dam breaches by visualizing flood wave depth and velocities. Sabeti et al. [15] created inundation maps of the Diyala River in northern Iraq using 2D HEC-RAS and ArcGIS. They anticipated their analysis would improve emergency readiness and evacuation planning in the event of a Darbandikhan dam collapse upstream of the river. Mihu-Pintilie et al. [16] reconstructed the 1968 River Chew flash flood by combining 2D hydraulic modeling with historical records like flood marks, photos, and

eyewitness reports. The study highlights the importance of advanced modeling and historical evidence in enhancing flood risk assessments where data are limited. Khudhur & Hamdan [17] reviewed the accuracy of 2D HEC-RAS hydraulic modelling for simulating a severe pluvial flash flood event in southeastern Romania using high-resolution LiDAR-derived DEMs, radar-based rainfall data, and post-event Synthetic Aperture Radar (SAR) imagery. Results showed a high degree of overlap (90–100%) between modelled and SAR-observed flood extents and a minimal error margin (less than ±0.3 m) for water depth measurements.

Several studies have shown that GIS, HEC-HMS, and HEC-RAS systems may be coupled to build effective flood models worldwide. Alrammahi & Hamdan [18] developed a rainfall-runoff model for a river in Iraq called the Diyala River Basin. Estimating infiltration losses was accomplished using the SCS-Curve Number method. Flow transformation was performed with the Clark Unit Hydrograph. For base flow, the recession technique was applied, and for channel routing, the Muskingum method was used. Model calibration and validation for the 2018–2019 period demonstrated high performance, with an R^2 value of 0.94. The study indicates the HEC-HMS model was very suitable for simulating runoff in the basin. Youssef et al. [19] performed a case study to assess the severe Al-Lith flood in Saudi Arabia following the dam failure. The research utilized HEC-HMS for rainfall-runoff simulation and HEC-RAS (2D) for flood inundation mapping. The WMS supported morphometric analysis and sub-basin identification, while HYFRAN performed rainfall frequency analysis. Satellite images from Landsat OLI and Sentinel-2, along with ArcGIS 10.5 and ERDAS, were used to support classification and spatial analysis.

The combination of field surveys and geospatial techniques enabled the practical assessment of flood hazards and the modeling of dam failure impacts. Ata et al. [20] developed a hydraulic and hydrological model for the Junjung River catchment in Penang, Malaysia, using HEC-HMS and HEC-RAS. This study identifies that combining HEC-HMS and HEC-RAS effectively identifies flood hazards and is essential for planning flood mitigation in rapidly growing watersheds. Alsubeai & Burckhard [21] and El-Bagoury & Gad [22] assessed the risk of flash floods in Saudi Arabia and Egypt using GIS data, HEC-HMS, and HEC-RAS. They used the SCS Unit Hydrograph to model surface runoff and the SCS-CN to quantify infiltration losses. The findings demonstrate that proactive flood prevention in arid regions is supported by combined HEC-RAS/HEC-HMS modeling, which also successfully forecasts floods and identifies risk zones. Supratman et al. [23] examined how land use affects flood dangers in Pondok Karya, Jakarta, Indonesia. The HEC-HMS and HEC-RAS tools with GIS were used to evaluate hydrological and hydraulic conditions for 25 discharge return periods using 2004–2021 daily rainfall data. Statistical and GIS methods developed the flood hazard index, which showed the Nash 0.65–Nash-Sutcliffe model efficiency (NSE). The study revealed that, despite vegetative cover exceeding 30%, the flood hazard increased, and soil properties and social factors influenced the performance of the inundation model.

The available literature recognizes the effective and accurate role of HEC-HMS, GIS, and HEC-RAS tools in flood risk assessment and analysis. Very few studies have been conducted on flood extension in Iraq, and there is no specific study that clarifies the extent of flooding in the Wasit watershed, which is under study.

Due to the limited hydrological and hydraulic studies for the Wasit Governorate, especially in the area under study, and to address the research gap, since the statistical analyses of annual rainfall data indicated a high likelihood of flood recurrence, with return periods from 2 to 50 years, the importance of flood prediction in Wasit Governorate becomes paramount in mitigating life-threatening risks, where this study aimed to develop an integration of HEC-HMS and HEC-RAS models for the Wasit watershed, the integration of a hydrological and hydraulic model to estimate the quantities of runoff by knowing the amount of rainfall, and to determine the flood extension. In the hydrological model, which was HEC-HMS, the Soil Conservation Service-Curve number (SCS-CN), SCS Unit Hydrograph, and Muskingum methods were used for loss, transformation, and routing calculations, respectively. In the hydraulic model, which was HEC-RAS, DEM was used to define the terrain in the area of study, and Manning roughness coefficients were defined by creating a land cover layer in RAS-Mapper and defining these coefficients. The flood was calculated in the area of study and compared with satellite images at the same time.

This catchment was selected because of the absence of recorded flow data for the watershed and the importance of this area, due to its proximity to the Tigris River, which is considered an important source of water for the middle and south of Iraq, so that it can connect the extra water from floods for mitigation.

Due to the lack of field data and the limited previous research, this study aims to develop a floodplain simulation model using hydraulic and hydrological techniques to simulate the flood that occurred in November 2015 in the study area, as shown in Figure 1.

The model's reliability and accuracy can be assessed by comparing the results with a corresponding satellite image at the same time. Additionally, by predicting the rainfall for any period by using artificial intelligence techniques and using these models for calculating the flood expansion, the model can assist decision-makers in implementing proactive measures, such as discharging the extra water for the nearest rivers to reduce flood risk. Moreover, the water could be stored in the wet season to benefit from it in the dry season.

Figure 1. Flooding of the study area in Wasit Governorate during the rainy period (November 2015)

2. Methodology

2.1. Study Area Description

Figure 2 shows the location of the study area in Wasit Governorate, which is in the center east of Iraq. The governorates of Diyala, Baghdad, Al-Qadisiyah, Dhi Qar, and Maysan border Wasit Governorate to the east, and the governorate has an eastern boundary with Iran. Data Access Viewer, POWER (https://power.larc.nasa.gov) shows that temperatures varied between 9.05 and 26.96°C and precipitation levels varied between 0 and 3.8 mm during the research period.

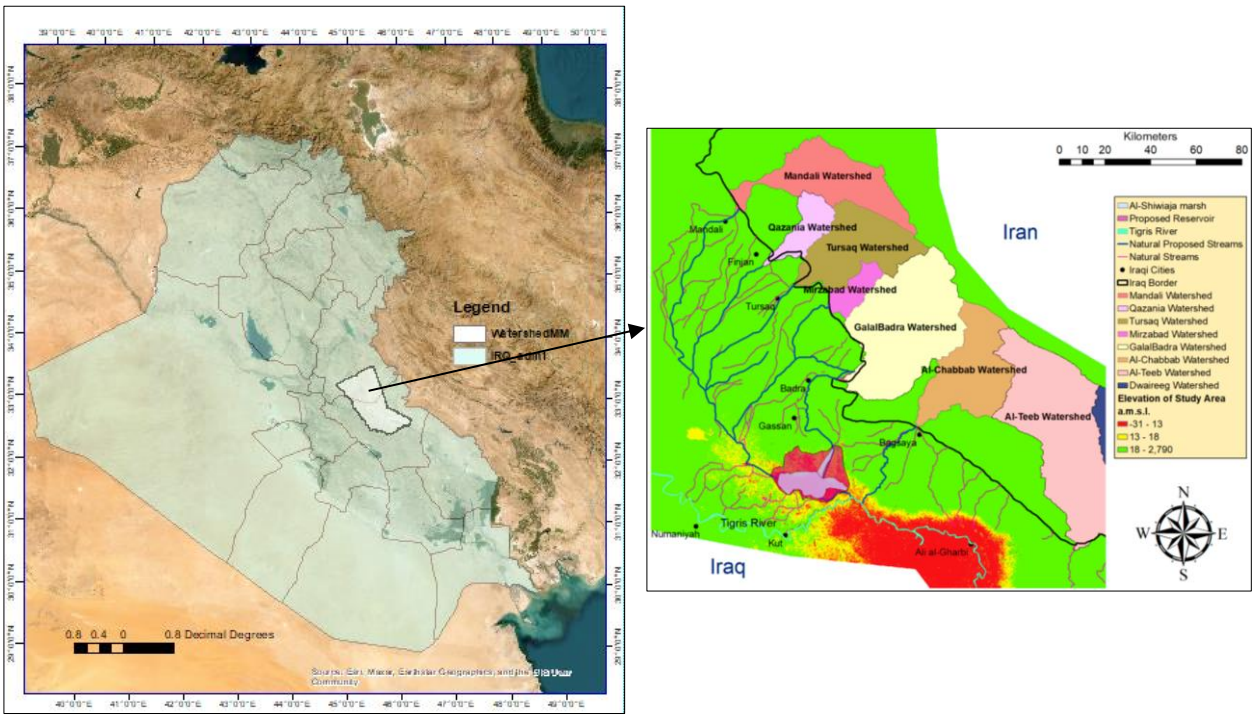

Figure 2. Area of study in Wasit Governorate, Iraq

To achieve the research objectives, various tools and materials were used. These tools included ArcMap (GIS) software to obtain hydrological and physical parameters, as well as spatial information for the study area. ArcMap was used as input to define watersheds and estimate their characteristics. In addition, the study included meteorological and hydrological data that had been obtained. Using HEC-HMS, we were able to model the transformation of precipitation into runoff in the watershed. To simulate the process of rainfall runoff in the watershed, HEC-HMS was used to enable the simulation of the conversion of rainfall to runoff. Furthermore, the HEC-RAS software was used for hydraulic analysis. The flowchart illustrated in Figure 3 showed the process of the methodology.

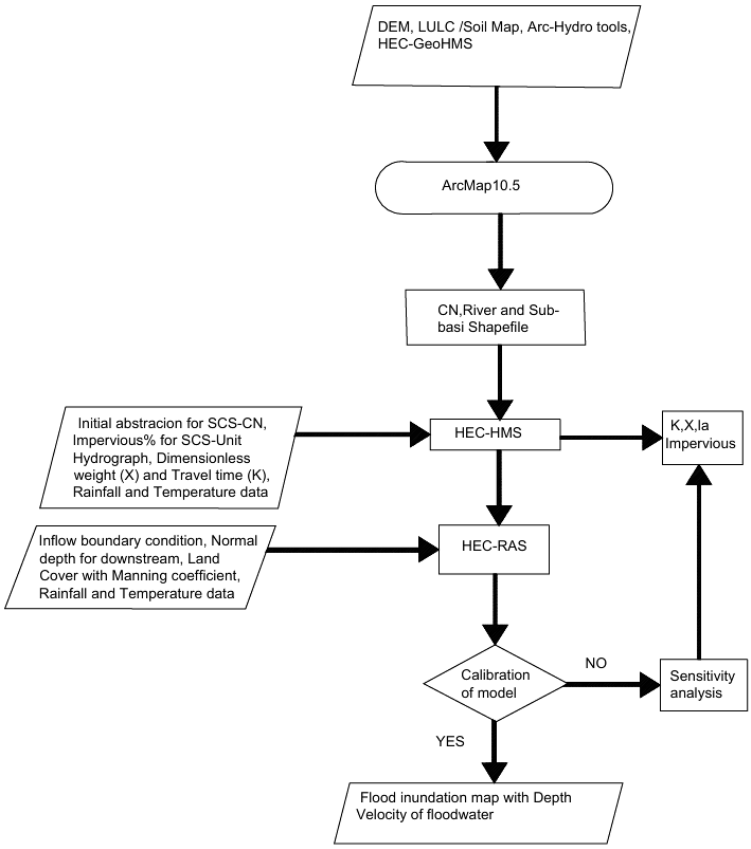

Figure 3. Flowchart for research methodology process

2.2. Geographic Information System (GIS)

For the purpose of creating accurately distributed flood risk maps over the flood site, the spatial modeling framework made use of GIS techniques and DEM [24]. The DEM created by the Shuttle Radar Topography Mission (SRTM) was obtained from the United States Geological Survey website (*https://earthexplorer.usgs.gov/*), and its spatial resolution for the areas under consideration was 30 meters. With the help of the Arc-Hydro tools built in ArcMap, the DEM was analyzed using GIS software (ArcMap 10.5), and from the DEM data and by using GIS, Hydrological variables, which include watershed delineation, flow direction, slope, length of the path, and watershed shape, were extracted.

2.3. HEC-Geo HMS

A hydrological extension toolbar within ArcGIS was utilized. Numerous hydrologic modelling inputs for HEC-HMS (*https://www.hec.usace.army.mil/software/hec-geohms/*) were generated using the Spatial Analyst extension and ArcGIS. One of the most vital hydrological parameters in modelling is the CN, which is essential for the prediction of surface runoff during or following rainfall events in the study area [25]. The model estimated hydrological factors and stream/sub-basin properties based on CN values.

2.4. Curve Number

The HEC-HMS model's CN grid file was derived from soil maps based on the Harmonized World Soil Database v2.0 (*https://www.fao.org/soils-portal/data-hub/soil-maps-and-databases/harmonized-world-soil-database-v20/en/*) and land use datasets from a 10-meter land cover map supplied by Microsoft, Esri, and Impact Observatory in GeoTIFF format. This composite of LULC from ESA Sentinel-2 images is accessible at *https://livingatlas.arcgis.com/landcoverexplorer/*. LULC and soil type data were imported into ArcGIS 10.5 to construct subbasin CNs.

2.5. HEC-HMS Model Description

Using conservation equations for mass, momentum, and energy, the HEC-HMS model describes many hydrological processes. It incorporates spatial and temporal variability and is valid for a wide range of situations [26]. Simulating the rainfall-runoff dynamics of dendritic watersheds is the aim of HEC-HMS 4.12. Runoff processes are modeled by connecting hydrologic elements within a dendritic network. The available elements include Diversion, Junction, Reach, and Sub basin. The process starts at an upstream element and flows downstream [27].

2.6. HEC-HMS Model Methods and Parameters

Hourly rainfall data and temperature were obtained from the NASA climate database (*https://power.larc.nasa.gov/data-access-viewer/*). The canopy was neglected due to the area under study was arid. Table 1 shows the hydrological model methodologies and parameters that were used in the modelling.

Table 1. Study area hydrological model methodologies and parameters

No.	Model	Technique	Required parameters (unit)
1	Loss Rate Parameter	SCS Curve Number	Initial abstraction (mm), CN, and Impervious area (%)
2	Run off Transform	SCS Unit Hydrograph	Lag Time (min)
3	Routing Method Constants	Muskingum	Dimensionless weight (X), and Travel time (K)

2.6.1. Loss Model (SCS-CN)

The volume of runoff is generally ascertained by deducting the water lost due to rainfall, which is estimated using loss models [28]. The direct runoff associated with a design rainfall was determined employing the SCS-CN method, which implemented the CN methodology for incremental losses [29]. The three parameters of the SCS-CN for the loss model are the initial abstraction (Ia), which defines the precipitation amount that falls before excess precipitation results, the CN, and the Impervious area (%), which was an important indicator of urbanization and built-up area size which used to explain the impact of urbanization on the hydrological response of the watershed. The SCS-CN method that was used in the loss model has been adopted for various regions and for various land uses and climatic conditions. It has been applied to a wide variety of applications beyond its original scope, including runoff estimation in large-scale river basins and integration in long-term, daily time-step, hydrological models [30]. The SCS needed a uniform procedure to estimate runoff throughout the country using available data without the need for calibration [31]. The CN values were determined by applying Equation 1 for every sub-basin [32]:

$$CN = \frac{\sum Ai\ CNi}{\sum Ai} \quad (1)$$

where CN_i denotes the corresponding CN, A_i denotes the sub-basin's area(km^2).

The potential abstraction S (mm), which is a function of CN, was determined by applying Equation 2.

$$S = \frac{25{,}400}{CN} - 254 \quad (2)$$

2.6.2. Transform Model (SCS Unit Hydrograph)

Additional rainfall becomes direct runoff using the transform model [33]. The study used the SCS Unit Hydrograph model (SCS-UH model) to transform additional rainfall into runoff. The SCS-UH simply requires the lag time, which is the period between the precipitation mass centroid and the runoff hydrograph peak point [7]. Lag time (min) was used in the Transform model with the SCS Unit hydrograph process. Lag time was determined by Equation 3 [32]:

$$Lag = \frac{(S+1)^{0.7} L^{0.8}}{1900 * Y^{0.5}} \quad (3)$$

where, Lag represents the basin lag time (hours), denoted as S, which is defined by Equation 2. It signifies the maximum retention (millimeters). Y indicates the slope of the basin (percentage), while L represents the catchment's hydraulic length (the longest flow path) measured in feet.

2.6.3. Routing Model (Muskingum)

The mathematical aspects of hydrologic flood routing are multi-faceted. Hydrologic routing is a method that uses approximations. It offers a less complicated option for dealing with flood routing issues. When planning flood mitigation for a river reach, the Muskingum method is among the most popular options. Storage and continuity equations are its basis [34]. Researchers have been paying close attention to the Muskingum technique for a number of reasons. As far as the specifics of the procedure are concerned, it is a straightforward approach that may be used for flood routing. The data from earlier floods may also be used to determine their parameters. Calibration utilizing experimental data relative to the extreme parts of the most substantially long stretches allows for a good enough reproduction of the phenomena that knowledge of the riverbed geometry is unnecessary [35]. There is no robust physical meaning to the dimensionless coefficient X, which must be between the integers 0.0 (highest attenuation) and 0.5 (no attenuation). The calibration process finds an intermediate value for the majority of stream reaches [5]. The time it takes for flood waves to traverse (Muskingum-k) is one of the other factors. The literature reports that the parameter K may range from one to five hours [33, 36].

2.7. HEC-RAS Model Description

Hydraulic modelling was executed utilizing the two-dimensional unsteady HEC-RAS software. Variations in floodwater depth over time were analyzed within the context of unsteady flow conditions [37]. The model configuration comprised three primary components: flow data, geometry data, and plan (control specification) data. Utilizing the integrated RAS mapper, HEC-RAS was capable of executing inundation mapping of the water surface.

2.7.1. Parameters of the Model

The following parameters were essential for running the HEC-RAS model:

- River and sub-basin shape files imported from HEC-HMS, Manning coefficient values were determined and assigned by adding "Land Cover map (satellite image with TIF file type) to the model as an additional layer, sourced from the Esri database (*https://livingatlas.arcgis.com/landcoverexplorer/*).
- The discharge from all tributaries was utilized as upstream boundary conditions and was computed using HEC-HMS. The boundary condition for the downstream was set using the normal depth.
- Cross sections and bank lines were created directly using HEC-RAS software through some steps in RAS Mapper.

A flow in which the elevation of floodwater has varied due to the variation in time represented the unsteady flow. The HEC-RAS model utilizes several hydraulics basics, particularly the Saint-Venant Equations for 2D unsteady flow [38]. It depended on mixing the two equations of diffusion wave and continuity in calculating the water level at a specific point and at a specific time, as shown in Equations 4 to 6 [24].

$$\frac{\partial H}{\partial t} + \frac{\partial (uh)}{\partial x} + \frac{\partial (vh)}{\partial y} + q = 0 \quad (4)$$

$$\frac{\partial H}{\partial t} + \nabla . hV + q = 0 \quad (5)$$

$$\nabla = \frac{\partial}{\partial x} + \frac{\partial}{\partial y} \quad (6)$$

where, H is the elevation of the water surface, h the depth of water, u and v the components of velocity in X and Y direction, V=f (u, v) as shown in Equations 7 [24].

$$V = -\frac{(R(H))^{\frac{2}{3}}}{n} \frac{\nabla H}{|\nabla H|^{\frac{1}{2}}} \quad (7)$$

where, R is the hydraulic radius, and n is the Manning's roughness coefficient.

2.7.2. Manning Roughness Coefficient

Manning's roughness coefficient, which was essential for the hydraulic model, were calculated and entered into RAS Mapper in two stages. First, a Land Cover image was obtained from the NASA website and added as a layer to RAS Mapper, as shown in Figure 4. The second step, as represented in Figure 5, involved adding Manning coefficient values to each land type on a required table.

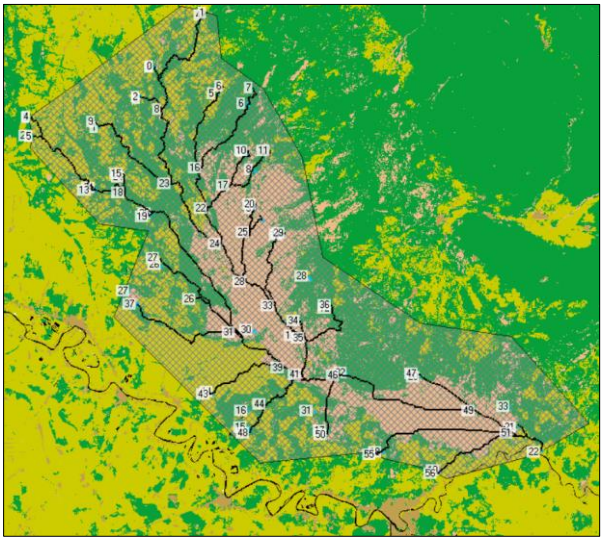

Figure 4. Land Cover Layer

Selected Area Edits

ID	Name	ManningsN	Percent Impervious
0	NoData	0.1	
11	Mixed Forest	0.1	
8	Grassland-Herbaceous	0.034	
5	Developed - Open Space	0.0404	
7	Pasture-Hay	0.325	
2	Developed - High Intensity	0.0404	
1	Unclassified	0.1	
4	Developed - Low Intensity	0.0678	
9	Deciduous Forest	0.36	

Figure 5. Manning's Roughness Values

2.8. Sensitivity Analysis

Sensitivity analysis was very important to evaluate the impact of changing the HEC-HMS hydrological model parameters on the hydrological simulation outputs in the study area, which represented the inputs for the HEC-RAS model. Due to the poverty of runoff records for adjusting the hydrological parameters in the area under study, the default values of the hydrological parameters were adjusted within acceptable limits based on values published in scientific literature and similar hydrological references.

A series of scenarios was executed using the HEC-HMS software, with each parameter being varied individually by a specific percentage. The sensitivity analysis process helped identify the most sensitive parameters in the modelling process, thus enhancing the reliability of the results in the absence of field observational data. In this study, the CN variable was excluded from the sensitivity analysis because of the results obtained using the method described in section 2.4.

2.9. The Model Calibration and Validation:

Calibration is a common technique employed to enhance model accuracy. The primary objective of calibration is to align the model output with observed data, which is accomplished through the adjustment of parameters and iterative evaluation of the results until the standard coefficients are satisfied. Validation must be used to evaluate the calibration process using periods other than those used to calibrate the model to prove its stability and validity. Due to conceivable of overfitting the model's parameters to the observed data during that time of calibration, the validation phase is essential for checking the calibration findings [39].

When studying areas with limited access to in-situ measurements, a mix of remote sensing and hydrodynamic modeling techniques might be useful. In a region where there is a lack of gauged data, this approach may be used to track the hydrodynamic processes during a flood event [40].

It has been challenging to calibrate the model with the absence of reliable observational and hydrological data, so the hydrological model has been calibrated by adjusting the hydrological factors through sensitivity analysis. The results of the inundation map were compared with the actual satellite photo (h*ttps://earthobservatory.nasa.gov/images/87011/flooding-in-iraq*) at the same time, which was November 14, 2015, using the Critical Success Index (CSI) [13, 41]. Gilbert (1884) [42] proposed this metric, which he dubbed the ratio of verification. Palmer & Allen (1949) [43] referred to it as the threat score, while Donaldson et al. (1975) [44] termed it the critical success index, or CSI [4]. Schaefer (1990) [45] remarked that it has been rediscovered and renamed at least twice. In order to locate the CSI, the simulated HEC-RAS 2D water surface and satellite image were categorized using ArcGIS after being transformed from polygons to raster layers [46]. Then, two raster layers were subtracted using the Raster calculator tool, and Equation 8 was used. The pixels that contain water are assigned a value of 255, whereas those that do not contain water are assigned a value of 0.

$$\mathrm{CSI} = \frac{\mathrm{Smod} \cap \mathrm{Sobs}}{\mathrm{Smod} \cup \mathrm{Sobs}} \times 100 \quad (8)$$

where Smod is the model's projected flooded surface area and Sobs is the satellite image's observed flooded surface area. A complete match between the regions predicted by the model and those flooded by satellite is indicated by a CSI-index value of 100, which may take values between 0 and 100%. To further investigate the model's propensity for under- or over-prediction, two further measures were additionally included in the study. Equations 9 and 10, which are respectively provided by Pertiwi et al. [40] and Wing et al. [47], were used to calculate the Hit Rate (HR) and the False Alarm (FAR) indices.

$$HR = \frac{Smod \cap Sobs}{Sobs} \times 100 \quad (9)$$

$$FAR = \frac{Smod - (Smod \cap Sobs)}{Smod} \times 100 \quad (10)$$

The values of both indices might be anything from zero to one hundred percent. A Hit Rate of 100 indicates that the model correctly predicted that all regions inundated by satellites were flooded; this percentage is expressed as a percentage of the total areas inundated by satellites. In contrast, the FAR of 0 indicates that no false alarms, and the FAR of 100% indicates all false alarms; the False Alarm index provides a sense of whether the model over-predicts the scope of the flood.

After carrying out the calibration steps by changing some of the most sensitive hydrological parameters, according to the mentioned sensitivity analysis, and achieving the accurate convergence between the simulation and reality, the model was verified by entering these confirmed and corrected parameters in the flood that occurred in April 2019, and ensuring the reliability of the model.

3. Results and Discussion

3.1. Results

The whole basin that divided into nine sub-basins that were formed from the basin, are shown in Table 2 and Figure 6, respectively. The following methods were used to calculate the runoff from these sub-basins: the SCS Unit Hydrograph method for loss estimation, the Muskingum method for transformation, and the SCS-CN methodology for routing calculations. After that, HEC-RAS was consulted to construct the hydraulic model using the expected runoff data. In order to create floodplain depth, velocity, and inundation maps, the Ras Mapper component of HEC-RAS was used. Certain hydrological and hydraulic parameters were obtained during the calibration process by comparing the simulated inundation map from HEC-RAS with a satellite image captured concurrently.

Table 2. The geographical coordinates and sub-basin areas of the study area

Sub-basin	Latitude	Longitude	Area (km^2)
W720	33.410604	45.254028	1,095.54
W940	33.304469	45.450336	810.02
W960	33.119314	45.558295	601.01
W1010	33.146256	45.144833	1,385.45
W1020	32.91551	45.264998	484.45
W1110	32.824412	45.539483	1,037.52
W1170	32.811257	45.846333	483.89
W1230	32.685118	45.623312	337.34
W1290	32.660422	45.914315	452.90

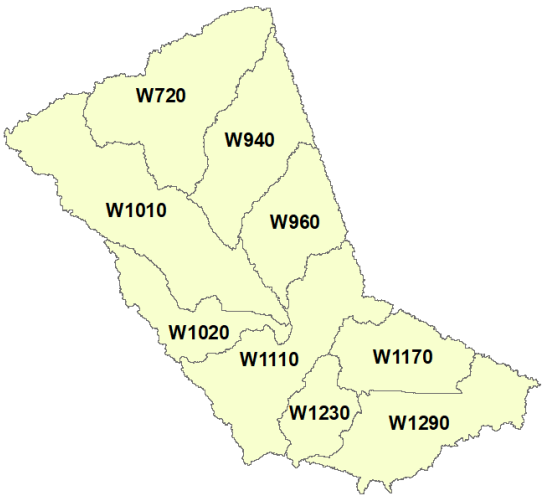

Figure 6. Area of study in Wasit Governorate

3.1.1. Digital Elevation Model (DEM)

Precise information for the research region was created using ArcMap software. As shown in Figure 7, eight DEM images describing the topography of the study area have been uploaded to ArcMap from the designated USGS location (*https://earthexplorer.usgs.gov*). One mosaic TIFF image was created by combining these eight TIFF-types DEMs using ArcMap, as shown in Figure 8. To represent the examined region and preliminary data for starting the initial stage of the hydrological model, the imported DEM was clipped to the precise area, as depicted in Figure 9. The spatial resolution of 30 m was used for generating the elevation map in Figure 10.

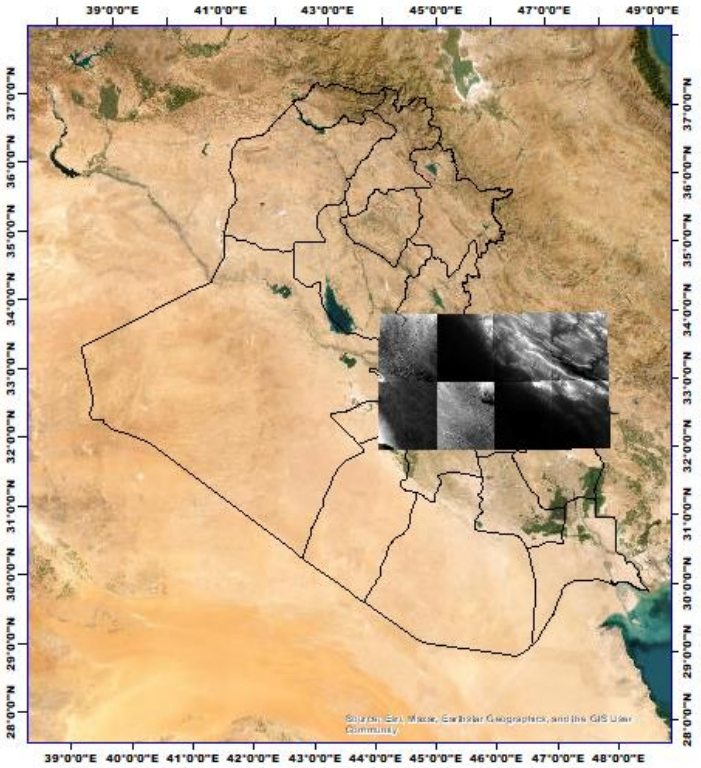

Figure 7. The eight DEM tiles (GeoTIFF format) used in the study

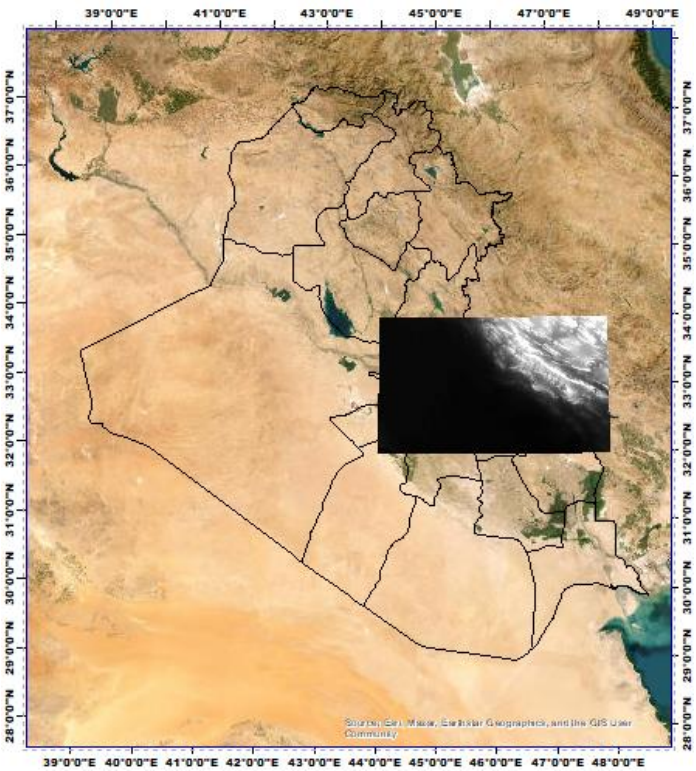

Figure 8. The merged DEM mosaic covering the study area

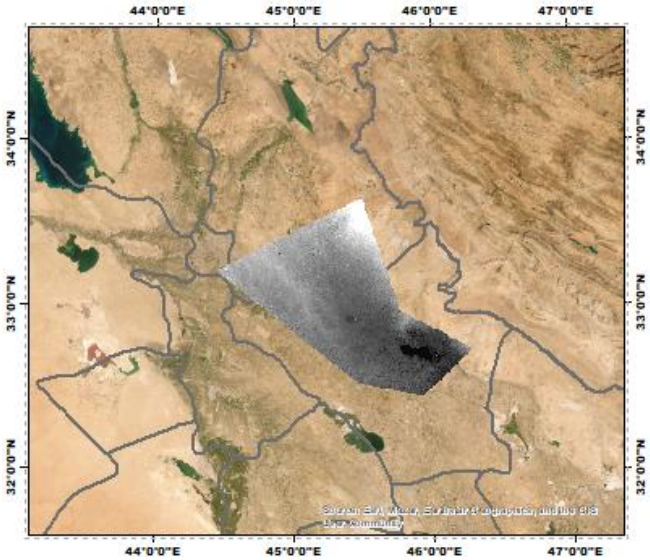

Figure 9. The clipped DEM representing boundaries of the research region

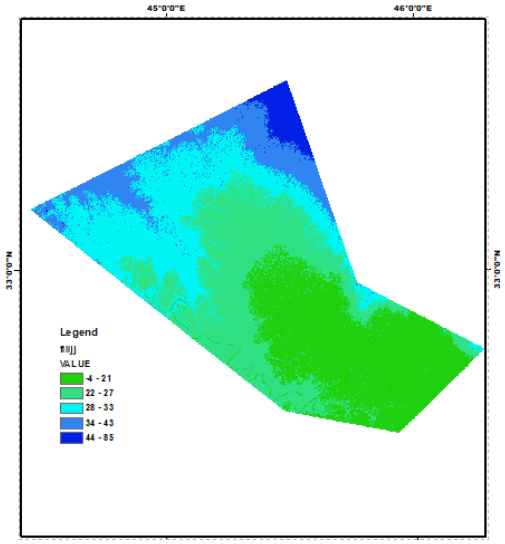

Figure 10. Elevation map of the research region

3.1.2. The Arc Hydro Tools

Multiple data sets describing the catchment drainage patterns were collected using Arc Hydro tools. Raster analysis generated data on fill sinks, the longest flow path, catchment polygon processing, catchment grid delineation, flow accumulation, drainage line processing, flow direction, slope, and watershed delineation. It was used of these data to create a vector of drainage representing networks and catchments. The geometric network presented in Figure 11 demonstrates how drainage lines and catchment areas are interconnected.

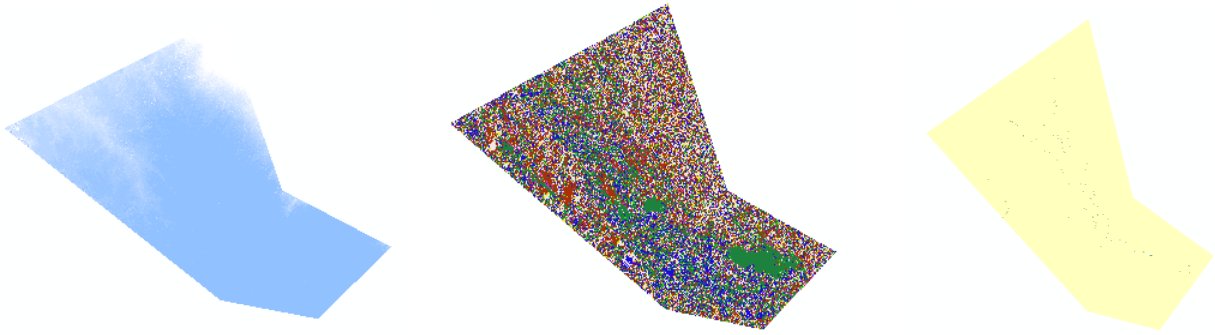

(a) (b) (c)

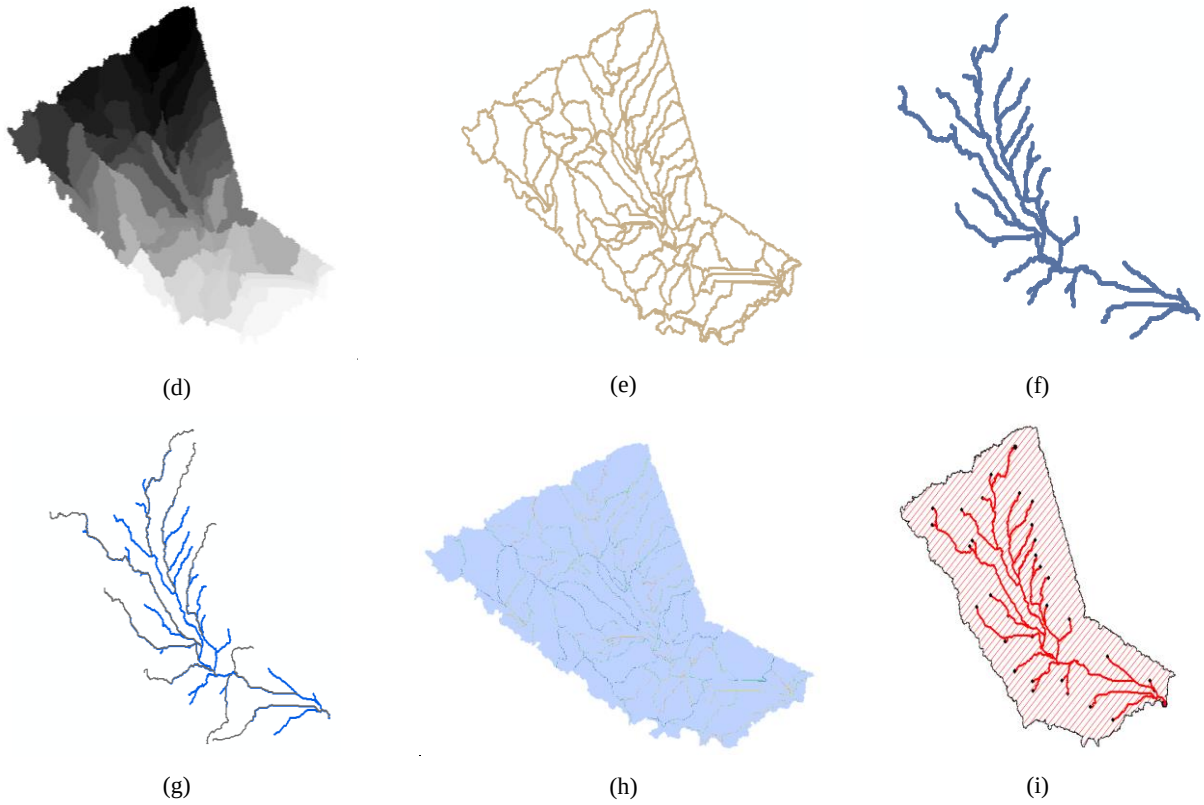

Figure 11. (a) Fill sink, (b) Flow Direction, (c) Flow Accumulation, (d) catchment grid delineation, (e) catchment polygon processing, (f) drainage line processing, (g) the longest flow path, (h) slope, (I) watershed delineation

3.1.3. HEC-GeoHMS

Model creation and terrain pre-processing were conducted using HEC-GeoHMS. Catchments were delineated, and parameters such as accumulation and flow direction were predicted. Additionally, sinks within the DEM were filled during the terrain pre-processing phase. The watershed boundaries were delineated and saved as shapefiles. The outlet points at 46.168753E and 32.646373N were established as a suitable outlet location. Following basin merging, as illustrated in Figure 12, the centroid of the basin and the HMS Link were identified. The resulting model was prepared for export to the HEC-HMS software platform. Furthermore, HEC-GeoHMS was utilized for additional processing steps, including the estimation of hydrologic parameters such as CNs.

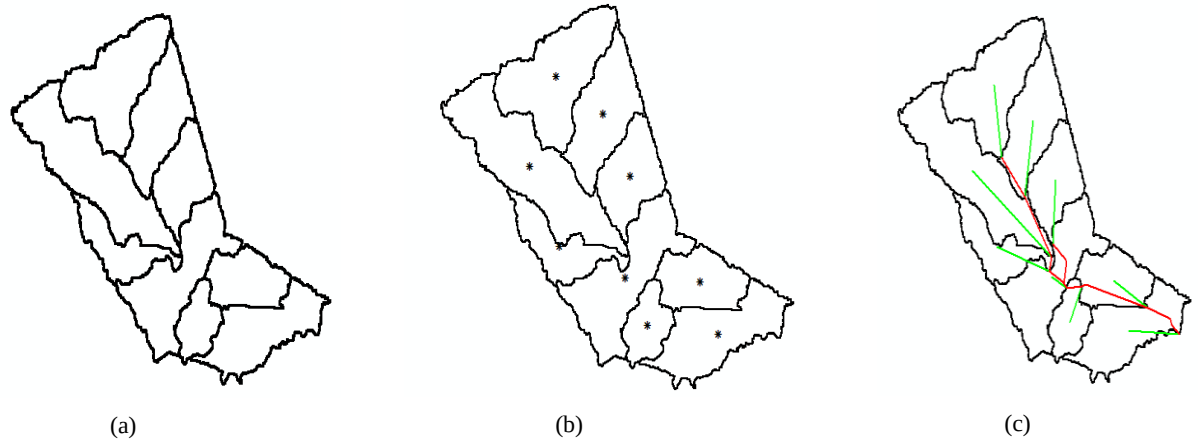

Figure 12. Model setup using HEC-GeoHMS: (a) Sub-basin, (b) Basin centroid, (c) HMS Link

3.1.4. Curve Number

To determine the CN for every subbasin, information on land use and soil types was used to generate it. Estimating the model's hydrological parameters and characterizing the watercourse or subbasin were both done using CN values [36, 48]. The process of calculating the CN values is shown in Figure 13.

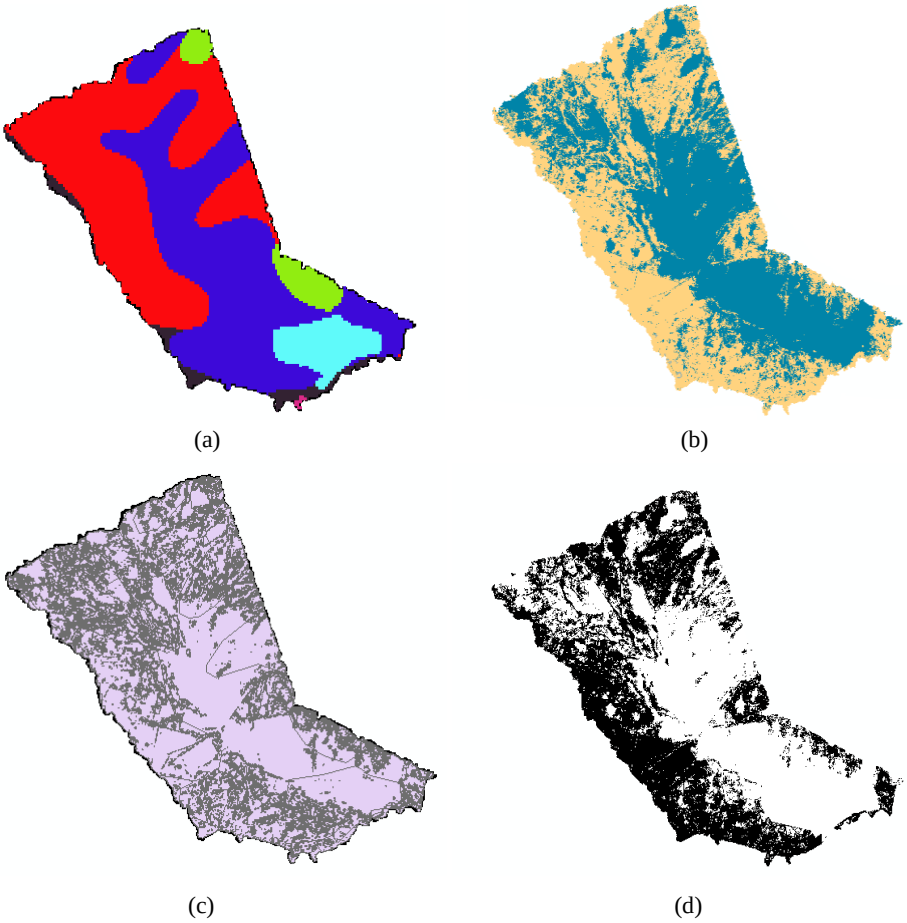

Figure 13. (a) soil map, (b) land use, (c) soil and LULC, (d) CN Grid

3.1.5. HEC-HMS

Following the model's pre-processing in HEC-GeoHMS, it was imported as a basin file into HEC-HMS. The rainfall-runoff processes of the catchment systems were modelled utilizing the HEC-HMS software. To operate the rainfall-runoff models, the meteorological model file and the hydrological parameters data are used as input in HEC-HMS during the rainfall-runoff process. The CN was estimated using the HEC-GeoHMS toolbox in ArcMap 10.5 [49]. This approximation is based on variables such as soil type, land use, and antecedent watershed moisture. Assuming the whole catchment was completely permeable, it was assumed that each sub-basin had an imperviousness rate of 0%. Some parameters incorporated into the basin model components include those related to sub-basins and reaches, such as loss parameters (percentage of imperviousness, initial abstraction, and CN), routing parameters (x and k), and transform parameters (lag time). The values of the basin lag time factors have been determined and converted to minutes during the operation of HEC-HMS. Table 3 shows the predicted values of the Loss and Transform Model's parameters.

Table 3. Estimates of parameter values for the Loss and Transform Model

Sub-basin	Area	CN	Potential maximum retention (S)	Initial abstraction (Ia) mm	Lag time (hr)
W720	1,095.54	79.39	2.596	13.19	32.037
W940	810.02	85.83	1.651	8.39	17.670
W960	601.01	97.61	0.245	1.24	8.974
W1010	1,385.45	84.199	1.877	9.53	10.731
W1020	484.45	73.95	3.523	17.90	10.729
W1110	1,037.52	79.21	2.625	13.33	7.526
W1170	483.89	94.34	0.600	3.05	3.640
W1230	337.34	81.68	2.243	11.39	7.363
W1290	452.90	88.10	1.351	6.86	3.459

In order to include precipitation and temperature data as time series, the time series data manager was used. Rainfall data was recorded from 5 November 2015 at 00:00 to 30 November 2015 at 00:00, with an hourly interval, in the case of the control run. For the research region, Figure 14 illustrates the HEC-HMS hydrological model.

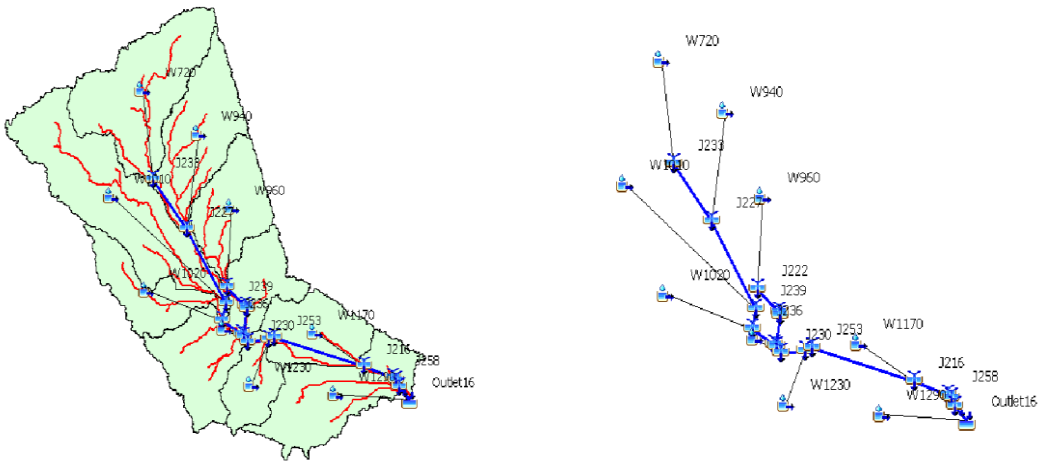

Figure 14. The hydrological model of the HEC-HMS for the research region

3.1.6. Sensitivity Analysis

Model sensitivity study revealed the impact of Ia, Muskingum K, and X, as well as impervious% factors, on model outputs and the reaction of different hydrological watershed features. By conducting a sensitivity analysis of Ia, we were able to better understand how soil properties and land use affect infiltration and surface runoff. This analysis had a small impact on the model, leading to very small percentage changes, but it did increase or decrease the impact by 30% to 50% of the default values. Low numbers at startup won't hurt the Hec-HMS model, but sensitivity showed up later on, and values will alter with time. A sensitivity study of impervious

% helps offer light on how urbanization affects the watershed's hydrological response. Regardless of its amount, it was shown that the impermeable percentage had an influence, although a little one. The model's dependence on other factors to provide realistic results, together with the reasonableness of the default choices, explains this. A sensitivity study of impervious% helps offer light on how urbanization affects the watershed's hydrological response. The impact of the river's characteristics on the hydrological response was helped to understand by the sensitivity analysis of Muskingum K and X. As shown in Figure 15, all four parameters don’t show an effective impact on the hydrological process before 19% increase.

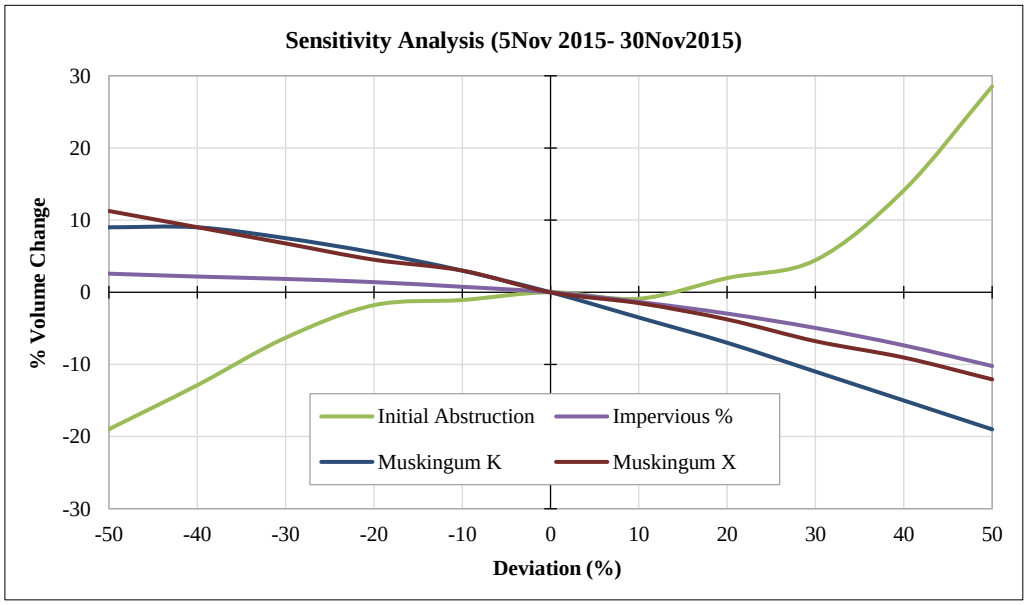

Figure 15. Sensitivity analysis (5 Nov 2015 - 30 Nov 2015)

3.1.7. HEC-RAS

The hydraulic simulation encompassed the period from November 5 to November 30, 2015, utilizing unsteady flow conditions and a flow hydrograph as a boundary input. A two-dimensional (2D) modeling approach was employed, where the size of the computational grid was selected to strike a balance between accuracy and

processing time. Boundary condition for every reach was added to enter the inflow, which was calculated by HEC-HMS to draw the flooded area. It commenced with the creation of the DEM in Ras Mapper and the delineation of river reaches and cross-sections, which ensured an accurate representation of channel geometry (see Figure 16). The ability to extract elevation values at each cross-section facilitated a precise assessment of flood depths across the study area. A smaller grid size enhances the model's accuracy but requires longer computational times. In this study, the smallest possible cell size was used, as further reducing the cell size would not affect the extent of the flooding. (see Figure 17). Then, after running, A match of the flooded area with the satellite image was checked. After calibration, a good match was achieved.

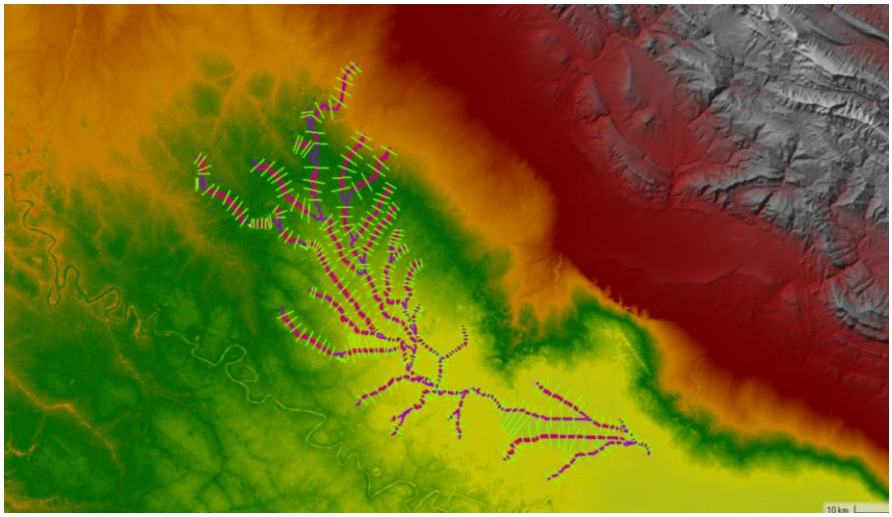

Figure 16. Created the RAS Mapper terrain, river reaches, and cross sections

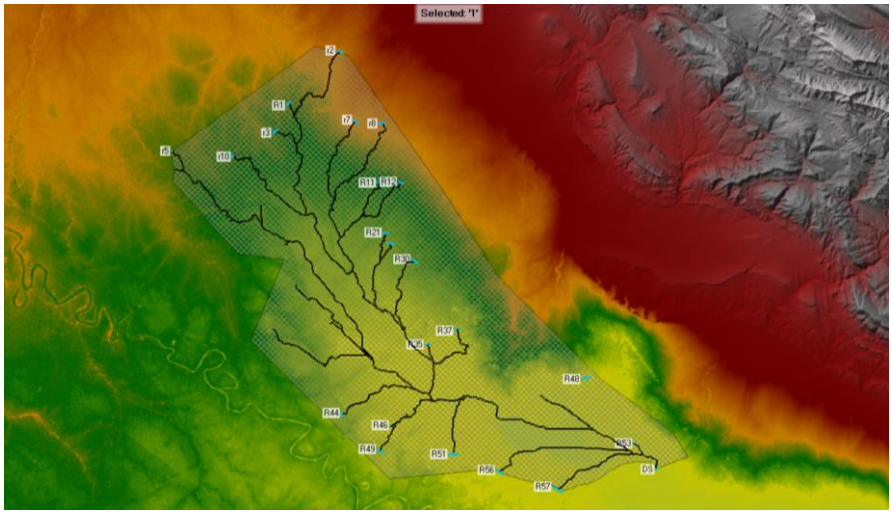

Figure 17. Created the polygon and Mesh size in the study area

3.1.8. The Model Calibration and Validation

The hydraulic model has been calibrated by adjusting the hydrological factors. The results of the inundation map were compared with the actual satellite photo (*https://earthobservatory.nasa.gov/images/87011/flooding-in-iraq*) at the same time, which was November 14, 2015, using CSI. The hydrological factors, Ia, Muskingum K, and X, and impervious% were adjusted using sensitivity analysis to achieve the greatest convergence between the model and satellite image. As shown in Figure 18, the result of CSI was 78.56%, (HR) was 95.31%, and (FAR)% was 8.33%. The study of Afzal et al. [13] used the CSI to assist the results of HEC-RAS simulation against satellite imagery-derived flood maps which achieved a high performance of the examined model's reality compared with the study simulation, producing CSI of 64% after calibration and 66% after validation. Figure 19 showed the validation results, which represented a good agreement between the simulated values and the satellite imagery data. The CSI for the validated model was 82.56%, (HR) was 96.62%, and (FAR)% was 10.01%. These results explained the efficiency and ability of the model to simulate 2019 data.

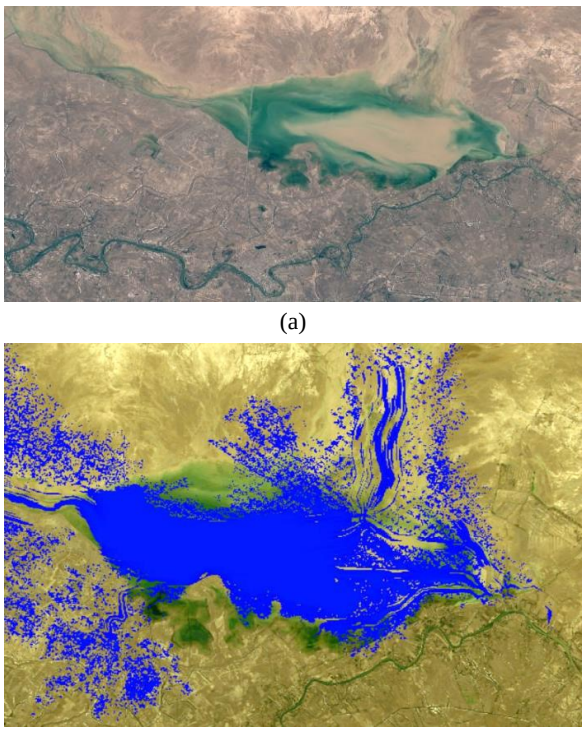

(a)

(b)

Figure 18. (a) Actual satellite image for flooding (November 14, 2015); (b) Hydraulic modeling image using HEC-RAS matching with the actual image (November 14, 2015): https://earthobservatory.nasa.gov/images/87011/flooding-in-iraq

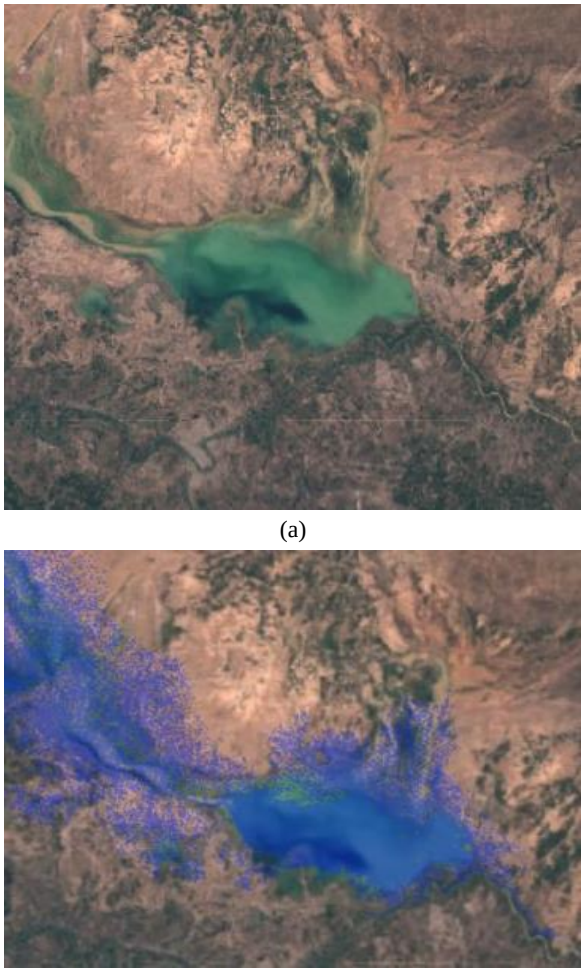

(a)

(b)

Figure 19. (a) Actual satellite image for flooding (April 3, 2019); (b) hydraulic modeling image using HEC-RAS matching with the actual image (April 3, 2019): https://earthmap.org/compare.html?geoJson/

3.1.9. Depth and Velocity

The hydraulic simulation was substantial in generating flood inundation maps by determining the floodwater depth and affected area. The floodwater depth and velocity maps, as shown in Figure 20, were classified into intervals using various colors to recognize the flood hazard areas.

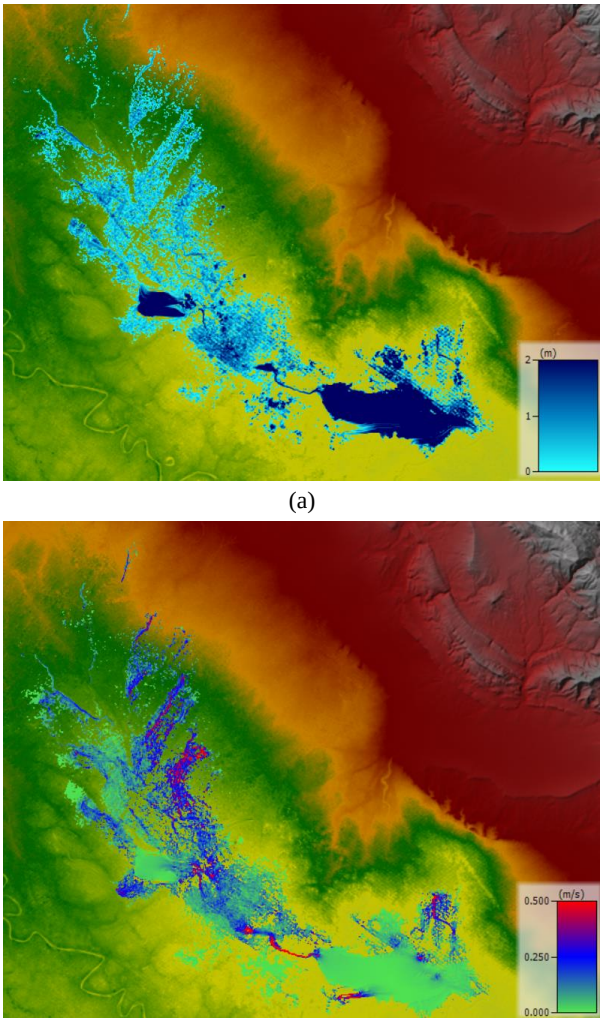

(a)

(b)

Figure 20. (a) The floodwater depth map; (b) The velocity of floodwater map

3.2. Discussion

In this research, the flood simulation was performed using GIS, HEC-HMS, and HEC-RAS. GIS was used to prepare the DEM. The results showed that increasing the spatial resolution cannot increase the accuracy of modeling the flood probability and may even decrease it at higher resolutions, consistent with some researchers' findings [50]. As the resolution of a DEM increases, the average slope of a watershed decreases, an effect known as "watershed flattening." Beyond a certain level of flattening, the accuracy of flood models and simulations decreases significantly, which is shown to be compatible with Zhu & Chen [51]. The land cover image used in the modeling was taken in the same year the flood occurred. Also, it was noticed that the region was arid, and there was little change shown to plant growth or death in the area of the study. In HEC-HMS, the preliminary attempt to execute the model was unsuccessful due to inconsistencies between the selected time interval and the lag time parameters. Adjusting the lag time to correspond with the model's temporal resolution enabled a more precise depiction of runoff. The successful execution of the simulation is shown to be compatible with Al-Zubaidi & Abed [52]. It proved the average CN value was 80.84 in Shuwaija Marsh, which represents the most important part of the study area. The comparison of this result with this study indicates the consistency and reality of it. Despite the data limitations in the study area, by using hydrological and hydraulic modelling, the validation methodology relied on a comparison between simulated flooding outcomes and satellite imagery, due to the absence of field data (such as flowrate gauge station in the area of the study), and to assess the reliability of the hydraulic model, the hydrological parameters of HEC-HMS model, K, X, Ia, and Improvise % were adjusted within a range located in the previous studies and the extent of its impact was determined through sensitivity

analysis, (Note that in this study, CN was fixed through specific equations and the values of the Manning coefficient were determined based on the nature of the land cover that was done by entering the land cover layer in RAS-Mapper, the Manning coefficient is determined from specific tables depending on the type of land cover.), after running HEC-HMS with suitable parameters and getting flow results then exported flow rates values to the HEC-RAS software and running the model then made a comparison of the flood results with a satellite image at the same time. The simulation results exhibited an acceptable level of agreement with satellite imagery using the CSI, indicating that the model effectively captured the observed flooding patterns. The slight differences in the CSI result are attributed to the accuracy of the DEM used and the simplification of some hydrological parameters within the HEC-HMS model.

The convergence observed through visual observations, in addition to the calculations with respect to CSI, gives an impression of the model's accuracy in arriving at the actual results, especially since the corrected hydrological values were adopted for verification in April 2019 and yielded a noticeable convergence between the calculated and observed results on 3 April 2019.

In flood risk management interpretation, these results give the importance of merging the meteorological prediction data with mitigation strategies. For instance, the lower areas could be preferred for generating drainage design or regulatory structures. Similarly, the areas that have the most inflow and limited infiltration capacity represent places to use monitoring or early warning systems. The low-lying areas of the floodplain exhibited better model performance compared to the high-lying areas and successfully reproduced the extreme flood event. Therefore, inundation modeling should always be conducted in conjunction with detailed meteorological prediction data for proper flood hazard warnings. In addition, due to water scarcity and drought in this region, especially in the summer, and the proximity of the flood zone to the Tigris River, it has become necessary to implement appropriate flood management and develop plans for water harvesting and how to exploit rainwater to benefit from it during times of drought.

4. Conclusion

This study effectively simulated the flood event in Wasit Governorate from 5 November 2015 to 30 November 2015 using the HEC-HMS and 2D HEC-RAS models. The flood results from RAS-Mapper in HEC-RAS were compared with satellite images after calibrating the hydrological parameters, yielding CSI = 88.56%, HR = 96.31%, and FAR = 8.33% for the flood on 14 November 2015. The calibrated hydrological parameters were then used to predict the flood on 3 April 2019, resulting in CSI = 82.56%, HR = 96.62%, and FAR = 10.01%, which demonstrate the high performance of the examined model compared with observed conditions at the same time. Knowledge of flood depth and velocity can help determine appropriate locations for installing discharge measurement and flood warning devices in flood-prone sub-basins.

The process of linking the hydrological model and the discharge values extracted from it, entering them as boundary conditions to the hydraulic model, conducting calibration and verification processes through them, and comparing them with satellite images at the time of the flooding showed good agreement. It can be proven, through integrating the two models, that the ability to know the extent of the flood and to benefit from this technology in predicting upcoming floods through forecasting rainfall to give notice to decision-makers to take precautions and be careful, and can also be used in rainwater harvesting projects. Accordingly, the study recommends the development of clear implementation mechanisms to ensure the effective and sustainable integration of model outputs into local planning and management plans.

5. Declarations

5.1. Author Contributions

Conceptualization, A.N.A.H and Y.T.Y.; methodology, A.N.A.H and Y.T.Y.; software, Y.T.Y.; validation, A.N.A.H and Y.T.Y.; formal analysis, Y.T.Y; investigation, Y.T.Y; resources, A.N.A.H and Y.T.Y.; data curation, Y.T.Y.; writing—original draft preparation, Y.T.Y.; writing—review and editing, A.N.A.H and Y.T.Y.; visualization, Y.T.Y.; supervision, A.N.A.H; project administration, A.N.A.H; funding acquisition, Y.T.Y. All authors have read and agreed to the published version of the manuscript.

5.2. Data Availability Statement

The data presented in this study are available on request from the corresponding author.

5.3. Funding

The authors received no financial support for the research, authorship, and/or publication of this article.

5.4. Conflicts of Interest

The authors declare no conflict of interest.

6. References

[1] Salih, R. A. K., Al-Juhaishi, M. R., Ibrahim, A. K., & Jabr, S. A. A. R. (2025). Statistical Analysis of the Maximum Annual Rainfall Data at Al-Shuwaija Marshes in Wasit Governorate, Iraq. Tikrit Journal of Engineering Sciences, 32(2), 22. doi:10.25130/tjes.32.2.22.

[2] Admas, M., Asrade, T. M., & Cherie, W. D. (2025). Application of the HEC-RAS and HEC-HMS Models for Flood Risk Analysis in the Gumara River, Upper Blue Nile Basin, Ethiopia. Advances in Meteorology, 2025(1), 5092932. doi:10.1155/adme/5092932.

[3] ReliefWeb. (2020). Flood hotspots in Iraq (October 2018-March 2019) (October 2020). ReliefWeb, New York, United States. Available online: https://reliefweb.int/map/iraq/flood-hotspots-iraq-october-2018-march-2019-october-2020 (accessed on December 2025).

[4] Chow, V. T., Maidment, D. R. & Mays, L. W. (1988) Applied Hydrology. International Edition, McGraw-Hill Book Company, New York, United States.

[5] HEC-HMS (2026). HEC-HMS User's Manual, USACE Hydrologic Engineering Center, Davis, United States. Available online: https://www.hec.usace.army.mil/confluence/hmsdocs/hmsum/4.12 (accessed on December 2025).

[6] Marimin, N. A., Razi, M. A. M., Ahmad, M. A., Adnan, M. S., & Rahmat, S. N. (2018). HEC-RAS hydraulic model for floodplain area in Sembrong River. International Journal of Integrated Engineering, 10(2), 151–157. doi:10.30880/ijie.2018.10.02.029.

[7] Salman, Q. M. K., & Hamdan, A. N. A. (2023). Runoff Estimation for the Central Region of the Lesser Zab River Watershed Using the SCS-Curve Number Method and GIS. Journal of Ecological Engineering, 24(9), 232–245. doi:10.12911/22998993/167789.

[8] Olayinka, D. N., & Irivbogbe, H. E. (2017). Estimation of Hydrological Outputs using HEC-HMS and GIS. Nigerian Journal of Environmental Sciences and Technology, 1(2), 390–402. doi:10.36263/nijest.2017.02.0054.

[9] Sagathia, J., Kotecha, N., Patel, H., & Patel, A. (2020). Impact Assessment of Urban Flood in Surat City using HEC-HMS and GIS. Proceedings of the 4th International Conference: Innovative Advancement in Engineering & Technology (IAET) 2020, 1-9. doi:10.2139/ssrn.3558360.

[10] Hamdan, A. N. A., Almuktar, S., & Scholz, M. (2021). Rainfall-runoff modeling using the HEC-HMS model for the Al-Adhaim river catchment, northern Iraq. Hydrology, 8(2). doi:10.3390/hydrology8020058.

[11] Kazezyılmaz-Alhan, C. M., Yalçın, Javanshour, K., Aytekin, M., & Gülbaz, S. (2021). A hydrological model for Ayamama watershed in Istanbul, Turkey, using HEC-HMS. Water Practice and Technology, 16(1), 154–161. doi:10.2166/wpt.2020.108.

[12] Hamdan, A. N. A., Abbas, A. A., & Najm, A. T. (2019). Flood hazard analysis of proposed regulator on Shatt Al-Arab River. Hydrology, 6(3), 80. doi:10.3390/hydrology6030080.

[13] Afzal, M. A., Ali, S., Nazeer, A., Khan, M. I., Waqas, M. M., Aslam, R. A., Cheema, M. J. M., Nadeem, M., Saddique, N., Muzammil, M., & Shah, A. N. (2022). Flood Inundation Modeling by Integrating HEC–RAS and Satellite Imagery: A Case Study of the Indus River Basin. Water (Switzerland), 14(19), 2984. doi:10.3390/w14192984.

[14] Mohamed, M. J., Karim, I. R., Fattah, M. Y., & Al-Ansari, N. (2023). Modelling Flood Wave Propagation as a Result of Dam Piping Failure Using 2D-HEC-RAS. Civil Engineering Journal (Iran), 9(10), 2503–2515. doi:10.28991/CEJ-2023-09-10-010.

[15] Sabeti, R., Stamataki, I., & Kjeldsen, T. R. (2024). Reconstructing the 1968 River Chew flash flood: merging a HEC-RAS 2D hydraulic modelling approach with historical evidence. Geomatics, Natural Hazards and Risk, 15(1), 2377655. doi:10.1080/19475705.2024.2377655.

[16] Mihu-Pintilie, A., Urzică, A., Stoleriu, C. C., & Pricop, C. I. (2025). Integrating LiDAR-derived DEM, rainfall radar data, and SAR imagery for 2D HEC-RAS modelling to assess the severity of pluvial flash floods induced by Storm Boris in SE Romania. Geomatics, Natural Hazards and Risk, 16(1), 2488190. doi:10.1080/19475705.2025.2488190.

[17] Khudhur, I. D., & Hamdan, A. N. A. (2024). Dam break modeling and downstream flood inundation mapping on Darbandikhan Dam, Iraq. Edelweiss Applied Science and Technology, 8(6), 6383-6403. doi:10.55214/25768484.v8i6.3382.

[18] Alrammahi, F. S., & Hamdan, A. N. A. (2022). Simulation of Rainfall-Runoff in the Diyala River Basin in Iraq using Hydrological Model by HMS with remote sensing, Geo-HMS and ArcGIS. IOP Conference Series: Earth and Environmental Science, 1120(1), 012007. doi:10.1088/1755-1315/1120/1/012007.

[19] Youssef, A. M., Abu-Abdullah, M. M., Abu Alfadail, E., Skilodimou, H. D., & Bathrellos, G. D. (2021). The devastating flood in the arid region a consequence of rainfall and dam failure: Case study, Al-Lith flood on 23th November 2018, Kingdom of Saudi Arabia. Zeitschrift Fur Geomorphologie, 63(1), 115–136. doi:10.1127/zfg/2021/0672.

[20] Ata, F. M., Toriman, M. E., Desa, S. M., San, L. Y., & Kamarudin, M. K. A. (2023). Development of Hydrological Modelling Using HEC-HMS and Hec-Ras for Flood Hazard Mapping At Junjung River Catchment. Planning Malaysia, 21(6), 116–129. doi:10.21837/PM.V21I30.1390.

[21] Alsubeai, A., & Burckhard, S. R. (2021). Rainfall-Runoff Simulation and Modelling Using HEC-HMS and HEC-RAS Models: Case Study Tabuk, Saudi Arabia. Natural Resources, 12(10), 321–338. doi:10.4236/nr.2021.1210022.

[22] El-Bagoury, H., & Gad, A. (2024). Integrated Hydrological Modeling for Watershed Analysis, Flood Prediction, and Mitigation Using Meteorological and Morphometric Data, SCS-CN, HEC-HMS/RAS, and QGIS. Water, 16(2), 356. doi:10.3390/w16020356.

[23] Supratman, M., Kusuma, M. S. B., Cahyono, M., & Kuntoro, A. A. (2024). Flood Hazard Assessment Due to Changes in Land Use and Cover. Civil Engineering Journal (Iran), 10(12), 3874–3891. doi:10.28991/CEJ-2024-010-12-04.

[24] HEC-RAS. (2016). HEC-RAS River Analysis System: User Manual 1D and 2D Version 5.0. Man. CPD-68. US Army Corps of Engineers Hydrologic Engineering Center, Davis, United States.

[25] Alrammahi, F. S. (2024). Estimation of curve number for hydrological models in the Northern area of Iraq. AIP Conference Proceedings, 3249(1), 0236578. doi:10.1063/5.0236578.

[26] Jehanzaib, M., Ajmal, M., Achite, M., & Kim, T. W. (2022). Comprehensive Review: Advancements in Rainfall-Runoff Modelling for Flood Mitigation. Climate, 10(10). doi:10.3390/cli10100147.

[27] U.S. Army Corps of Engineers, Hydrologic Engineering Center. (2024). HEC-HMS Hydrologic Modeling System: User's Manual (Version 4.13). US Army Corps of Engineers Hydrologic Engineering Center, Davis, United States. Available online: https://www.hec.usace.army.mil/software/hec-hms/ (accessed on December 2025).

[28] Goodarzi, M. R., Poorattar, M. J., Vazirian, M., & Talebi, A. (2024). Evaluation of a weather forecasting model and HEC-HMS for flood forecasting: case study of Talesh catchment. Applied Water Science, 14(2), 34. doi:10.1007/s13201-023-02079-x.

[29] HEC:USACE (2026). Curve Number, HEC-RAS Hydraulic Reference Manual. US Army Corps of Engineers Hydrologic Engineering Center, Davis, United States.

[30] Soulis, K. X. (2021). Soil conservation service curve number (SCS-CN) method: Current applications, remaining challenges, and future perspectives. In Water (Switzerland) (Vol. 13, Issue 2). doi:10.3390/w13020192.

[31] Williams, J. R., Kannan, N., Wang, X., Santhi, C., & Arnold, J. G. (2012). Evolution of the SCS Runoff Curve Number Method and Its Application to Continuous Runoff Simulation. Journal of Hydrologic Engineering, 17(11), 1221–1229. doi:10.1061/(asce)he.1943-5584.0000529.

[32] Souley Tangam, I., Yonaba, R., Niang, D., Adamou, M. M., Keïta, A., & Karambiri, H. (2024). Daily Simulation of the Rainfall–Runoff Relationship in the Sirba River Basin in West Africa: Insights from the HEC-HMS Model. Hydrology, 11(3), 34. doi:10.3390/hydrology11030034.

[33] Martin, O., Rugumayo, A., & Ovcharovichova, J. (2012). Application of HEC-HMS / RAS and GIS Tools in Flood Modeling : A Case Study for River Sironko – Uganda. Global Journal of Engineering, Design & Technology, 1(2), 19–31.

[34] Alhumoud, J. (2022). Analysis and Evaluation of Flood Routing using Muskingum Method. Journal of Applied Engineering Science, 20(4), 1366–1377. doi:10.5937/jaes0-37455.

[35] Alhumoud, J., & Almashan, N. (2019). Muskingum Method with Variable Parameter Estimation. Mathematical Modelling of Engineering Problems, 6(3), 355–362. doi:10.18280/mmep.060306.

[36] Natakusumah, D. K., Hatmoko, W., Harlan, D., Nugroho, E. O., Kuntoro, A. A., Farid, M., … Javas, J. (2025). The ITB Unit Hydrograph Method: A Novel Approach to User-Defined Unit Hydrograph Development (Part II). Civil Engineering Journal, 11(5), 1980–2007. doi:10.28991/CEJ-2025-011-05-015.

[37] Phyo, A. P., Yabar, H., & Richards, D. (2023). Managing dam breach and flood inundation by HEC-RAS modeling and GIS mapping for disaster risk management. Case Studies in Chemical and Environmental Engineering, 8. doi:10.1016/j.cscee.2023.100487.

[38] HEC:USACE (2026). HEC-RAS River Analysis System: User Manual 1D and 2D Version 5.0, US Army Corps of Engineers Hydrologic Engineering Center, Davis, United States. Available online: www.hec.usace.army.mil (accessed on January 2026).

[39] Palaić, D., Štajduhar, I., Ljubic, S., & Wolf, I. (2023). Development, Calibration, and Validation of a Simulation Model for Indoor Temperature Prediction and HVAC System Fault Detection. Buildings, 13(6). doi:10.3390/buildings13061388.

[40] Pertiwi, A. P., Roth, A., Schaffhauser, T., Bhola, P. K., Reuß, F., Stettner, S., Kuenzer, C., & Disse, M. (2021). Monitoring the spring flood in Lena delta with hydrodynamic modeling based on SAR satellite products. Remote Sensing, 13(22), 4695. doi:10.3390/rs13224695.

[41] Zotou, I., Karamvasis, K., Karathanassi, V., & Tsihrintzis, V. A. (2022). Potential of Two SAR-Based Flood Mapping Approaches in Supporting an Integrated 1D/2D HEC-RAS Model. Water, 14(24), 4020. doi:10.3390/w14244020.

[42] Gilbert, G. K. (1884). Finley's tornado predictions. American Meteorological Journal, 1, 166–172.

[43] Palmer, W. C., & Allen, R. A. (1949). Note on the accuracy of forecasts concerning the rain problem. United States Weather Bureau, Maryland, United States.

[44] Donaldson, R. J., Dyer, R. M., & Kraus, M. J. (1975). An objective evaluator of techniques for predicting severe weather events. Preprints, Ninth Conference on Severe Local Storms, 321326.

[45] Schaefer, J. T. (1990). The critical success index as an indicator of warning skill. Weather and Forecasting, 5(4), 570-575.

[46] Elkhrachy, I., Pham, Q. B., Costache, R., Mohajane, M., Rahman, K. U., Shahabi, H., Linh, N. T. T., & Anh, D. T. (2021). Sentinel-1 remote sensing data and Hydrologic Engineering Centres River Analysis System two-dimensional integration for flash flood detection and modelling in New Cairo City, Egypt. Journal of Flood Risk Management, 14(2), 12692. doi:10.1111/jfr3.12692.

[47] Wing, O. E. J., Bates, P. D., Sampson, C. C., Smith, A. M., Johnson, K. A., & Erickson, T. A. (2017). Validation of a 30 m resolution flood hazard model of the conterminous United States. Water Resources Research, 53(9), 7968–7986. doi:10.1002/2017WR020917.

[48] Tassew, B. G., Belete, M. A., & Miegel, K. (2019). Application of HEC-HMS Model for Flow Simulation in the Lake Tana Basin: The Case of Gilgel Abay Catchment, Upper Blue Nile Basin, Ethiopia. Hydrology, 6(1), 21. doi:10.3390/hydrology6010021.

[49] Belay, Y. Y., Gouday, Y. A., & Alemnew, H. N. (2022). Comparison of HEC-HMS hydrologic model for estimation of runoff computation techniques as a design input: case of Middle Awash multi-purpose dam, Ethiopia. Applied Water Science, 12(10), 237. doi:10.1007/s13201-022-01764-7.

[50] Avand, M., Kuriqi, A., Khazaei, M., & Ghorbanzadeh, O. (2022). DEM resolution effects on machine learning performance for flood probability mapping. Journal of Hydro-Environment Research, 40, 1–16. doi:10.1016/j.jher.2021.10.002.

[51] Zhu, H., & Chen, Y. (2024). A Study of the Effect of DEM Spatial Resolution on Flood Simulation in Distributed Hydrological Modeling. Remote Sensing, 16(16), 3105. doi:10.3390/rs16163105.

[52] Al-zubaidi, S. A., & Abed, B. S. (2024). Studying and Assessing Surface Water Use of Shuwaija Marsh within Wasit Governorate-Iraq. Journal of Engineering, 30(03), 159–176. doi:10.31026/j.eng.2024.03.11.